Journal of Statistical Physics, Vol. 85, Nos. 5/6, 1996

Energy Level Statistics in Disordered Metals with an Anderson Transition

S. N. Evangelou[1,2] and D. E. Katsanos[1]

Received September 5, 1995; final February 22, 1996

We present numerical scaling results for the energy level statistics in orthogonal and symplectic tight-binding Hamiltonian random matrix ensembles defined on disordered two and three-dimensional electronic systems with and without spin–orbit coupling (SOC), respectively. In the metallic phase for weak disorder the nearest level spacing distribution function $P(S)$, the number variance $\langle(\delta N)^2\rangle$, and the two-point correlation function $K_2(\varepsilon)$ are shown to be described by the Gaussian random matrix theories. In the insulating phase, for strong disorder, the correlations vanish for large scales and the ordinary Poisson statistics is asymptotically recovered, which is consistent with localization of the corresponding eigenstates. At the Anderson metal–insulator transition we obtain new universal scale-invariant distribution functions describing the critical spectral density fluctuations.

KEY WORDS: Anderson localization; spin–orbit coupling; mobility edge; random matrix theory; level statistics.

1. INTRODUCTION

The fundamental problem of electronic structure in disordered quantum systems is commonly studied within the tight-binding approximation.[1] The corresponding statistical tight-binding random matrix ensemble (TBRME) has been widely studied since the realization made by Anderson[2] that eigenvectors may show exponential decay properties in the presence of disorder. This is the well-known phenomenon of Anderson localization which occurs via the disorder-induced metal–insulator transition. The Anderson delocalization–localization transition is expected to occur in three-dimensional noninteracting disordered systems[3] and in two dimensions only when strong spin–orbit coupling (SOC) is also present.[4] In this

[1] Department of Physics, University of Ioannina, Ioannina, 45 110, Greece.
[2] Institute for Electronic Structure & Lasers, FORTH, Heraklion, P.O. Box 1527, Crete, Greece.

822/85/5-6-1

paper we shall work from the viewpoint of the Hamiltonian random matrix statistical approach by considering two kinds of tight-binding random matrices, both invariant under time reversal with and without SOC, corresponding to the orthogonal and the symplectic universality classes, respectively.[3] Our purpose is to characterize the statistical eigenvalue correlations and fluctuations, to identify the common features of the two quantum phase transitions and connect our results to the more general field of random matrix theories.

It is well established by now that the statistical properties of the energy spectra for diffusing electrons in the disordered metallic phase, studied within the TBRME, consist of correlated eigenvalues which resemble those found from appropriate Gaussian random matrix ensembles.[5,6] This description is usually referred as the Wigner–Dyson random matrix theory (RMT)[5,6] and is also believed to apply to nonrandom quantum systems whose classical dynamics is chaotic.[7] The correlations in this case arise because the eigenfunctions are delocalized, overlapping with each other, so that the corresponding eigenvalues exhibit level repulsion, giving a smooth and rigid spectrum. This kind of statistics is also known as a mesoscopic description since is it responsible for the universal mesoscopic conductance fluctuations in disordered metals.[8] In the insulating phase the eigenfunctions are instead localized nonoverlapping in space and imply uncorrelated spectra with randomly distributed eigenvalues obeying normal Poisson statistics. The analogy of delocalization (metal) to Wigner–Dyson and localization (insulator) to Poisson statistics is quite rigorous and has been exploited to define the mobility edge as the point in the energy spectrum where the eigenvalues change their statistics.[9–11]

The simplest quantity which can be used to unravel the statistical localization properties of these systems is the nearest-level spacing distribution function $P(S)$, which is defined so that $P(S)\,dS$ measures the probability of having a spacing in the interval $[S, S+dS]$. In order to have dimensionless quantities the spacing S is measured in units of the mean level spacing $\langle S\rangle = \Delta$. For delocalized eigenfunctions $P(S)$ obeys the well-known Wigner surmise, which in the orthogonal case takes the form $P(S) = (\pi/2)\,S \exp[-(\pi/4)\,S^2]$ and in the symplectic case is $P(S) = (2^{18}/3^6\pi^3)\,S^4 \exp[-(64/9\pi)\,S^2]$. These laws are derived from the Gaussian orthogonal ensemble (GOE) and the Gaussian symplectic ensemble (GSE), respectively.[5] For localized eigenstates both expressions cross over to the usual Poisson law $P(S) = \exp(-S)$. The main difference between the Wigner and the Poisson laws lies in the fact that for short separations S the Wigner surmise vanishes, indicating level repulsion with the first ($\beta = 1$) and the fourth power ($\beta = 4$) of S for the orthogonal and the symplectic universality classes, respectively. The parameter β is a universality class index

which reduces to zero in the Poisson case since $P(S)$ reaches its maximum value for $S=0$. A very interesting question also concerns the nature of the $P(S)$ function at the Anderson transition. The existence of a new universal critical statistics, intermediate between Wigner and Poisson, was first suggested and demonstrated in the pioneering work of ref. 10. The critical $P(S)$ distribution was computed for the orthogonal case and in general is shown to be a scale invariant function which displays Wigner-like behavior ($\propto S^{\beta}$) for small S falling off as a stretched exponential $\propto \exp(-AS^{\alpha})$, $A=$ const., for large S, where the exponent α is not far from unity (see also ref. 11), so that $P(S)$ for very large S is close to a simple exponential Poissonic behavior.[10]

In this paper we consider the kind of spectral correlations and fluctuations which appear in both the metal and insulator as well as at the mobility edge in two- and three-dimensional disordered systems which display an Anderson transition. We are also able to evaluate long-range correlations between eigenvalues, which give extra information on the spectral fluctuations not revealed by the $P(S)$ function. Therefore, in order to have a more complete description apart from $P(S)$ we extend our studies to the more fundamental statistical measures of the number variance $\langle(\delta N)^2\rangle$ and the density–density correlation function $K_2(\varepsilon)$. The number variance $\langle(\delta N)^2\rangle$ measures the fluctuations due to disorder in the number of levels within a given band of width E, with a mean number of levels $\langle N\rangle$. According to the Wigner–Dyson RMT for the metal $\langle(\delta N)^2\rangle$ is expected to vary logarithmically with $\langle N\rangle$ as

$$\langle(\delta N)^2\rangle = \frac{2}{\pi^2}\left[\ln(2\pi\langle N\rangle) + 2.18\right]$$

and

$$\langle(\delta N)^2\rangle = \frac{1}{2\pi^2}\left[\ln(4\pi\langle N\rangle) + 4.65\right]$$

up to order $1/\langle N\rangle$ for the two ensembles, while for the insulator, ordinary Poisson statistics $\langle(\delta N)^2\rangle = \langle N\rangle$ should be recovered. In other words, in the metallic phase the fluctuations are very small [$\propto (1/\beta)\ln\langle N\rangle$] when compared to the insulator ($\propto \langle N\rangle$), due to the presence of level repulsion in the former case. The logarithmic d-independent RMT expressions for a finite system should hold up to the mean value of $\langle N(E_T)\rangle = E_T/\Delta = g$, where g is the conductance in units of e^2/h and $E_T = h/\tau$ defines the characteristic Thouless energy, with τ the time it takes for the electron to diffuse through the sample. The applicability of the RMT is restricted to the energies $E \ll E_T$. The larger $E \gg E_T$ denotes a nonergodic diffusive metallic

regime, which is unreachable in the infinite metallic system, where the number variance scales as $(E/E_T)^{d/2}$ in d dimensions.[8,9] The insulating regime for systems of linear sizes L much larger than ξ can be understood from a random superposition of $(L/\xi)^d$ metallic subsystems of volume ξ^d each, which results in independent Poisson statistics.

An even more rigorous spectral fluctuation measure is the density–density correlation function $K_2(\varepsilon)$ which is appropriate to describe correlations of two energies at a distance ε apart, by removing lower order correlations. It is also related to the probability of finding two eigenvalues with a distance ε between them. The corresponding expressions for $K_2(\varepsilon)$ are shown here to be approximated by the Wigner–Dyson RMT[6] for the metal and to approach zero for the insulator. Apart from the general demonstration of the validity of the Wigner–Dyson and the Poisson statistics in the metallic and insulating limits, respectively, we obtain novel universal $\langle(\delta N)^2\rangle$ and $K_2(\varepsilon)$ curves for the two TBRMEs at the critical point. These new distributions describe even more accurately the level density fluctuations at the mobility edge. Moreover, our numerical scaling results are discussed according to a recent level statistical theory[12–15] which gives the asymptotics of $\langle(\delta N)^2\rangle$ and $K_2(\varepsilon)$ in the critical regime. It must be pointed out that although we deal with finite size systems our concern is the thermodynamic limit ($L \to \infty$) where the only energy scale is Δ and the metallic, insulating and critical asymptotic distributions should characterize the level fluctuations.

We proceed as follows: In Section 2 we introduce the orthogonal and symplectic matrix ensembles in the corresponding space dimensionalities. In Section 3 we show our results for $P(S)$, $\langle(\delta N)^2\rangle$ and $K_2(\varepsilon)$ in the metallic, insulating, and critical regimes for the orthogonal case in $d=3$. Our exposition of the results for the statistical spectral fluctuation measures in the less-studied $d=2$ spin-dependent symplectic case is undertaken in Section 4, also by using an alternative tranfer matrix scaling technique to locate the transition point. Finally, in Section 5 we discuss our results and derive the main conclusions drawn from our study.

2. THE TIGHT-BINDING RANDOM MATRIX ENSEMBLES

The first kind of matrices where randomness plays an important role are the Gaussian random matrices. They were introduced in the context of nuclear physics by Wigner and Dyson[5] in order to replace complicated many-body Hamiltonians by ignoring the details and keeping only the correct symmetries. They can be classified according to symmetry into three universality classes, with the most common example that of real and symmetric matrices which correspond to the orthogonal case defined by the

GOE. The SOC causes a crossover to the symplectic universality class where the random matrices become spin-dependent complex Hermitian quaternion-like and correspond to the GSE.[5] The Gaussian random matrices have all the matrix elements as independent identically distributed random variables, chosen from a Gaussian probability distribution of mean zero and fixed variance.

The GOE and GSE are exactly solvable for both the ensemble-averaged properties, such as the averaged density of states $\langle \rho(E) \rangle$, which for the GOE obeys a simple semicircle law, and also for the corresponding level fluctuations, e.g., the nearest-level spacing distribution function $P(S)$ obeys the Wigner surmise. The GOE and GSE limits should be approached from the appropriate TBRMEs without and with SOC, respectively, only for $d = \infty$ when both the diagonal (ε_n) and off-diagonal ($V_{n,m}$) matrix elements are random variables being, somehow, a mean-field limit of the TBRME. They can be also viewed as a zero-dimensional ergodic limit. However, for weak disorder, when the TBRME has random delocalized states, all the results from the GOE add GSE can carry through, reasonably explaining the measurable fluctuation phenomena in metallic conductors of size smaller than other characteristic decay lengths.

2.1. The Spinless Orthogonal Case in $d = 3$

Anderson localization can be studied via the dimensionality-dependent TBRME.[1] In the absence of spin effects the TBRME consists of real and symmetric random matrices but of drastically different structure than those of the GOE. They are short-ranged and sparse, reflecting the finite range of the interactions and in $d = 3$ are defined by the Hamiltonian

$$\mathbf{H} = \sum_{n,\sigma} \varepsilon_n |n\rangle\langle n| + \sum_{(n,m)} V_{n,m} |n\rangle\langle m| \tag{1}$$

where n labels all the L^3 sites of a three-dimensional lattice with linear size L, while the second sum is taken over all nearest neighbor pairs (n, m) on the lattice.

In our calculations we deal with finite samples with periodic boundary conditions and the spectrum of the exact electron states is discrete. The random on-site potential ε_n denotes the diagonal disorder and is a uniformly distributed random variable, between $-W/2$ to $W/2$, while the off-diagonal matrix elements $V_{n,m}$ are constant ($V_{n,m} = 1$). The Anderson transition for the $E = 0$ eigenfunctions occurs for a critical disorder $W_c \simeq 16.5$ in $d = 3$ and the states become localized for $W > W_c$. For a fixed amount of disorder $W = 12$ the critical energy (mobility edge) is at $E_c \approx 7.8$.[16]

2.2. The Spin-Dependent Symplectic Case in $d=2$

For a two-dimensional disordered system which contains SOC for spin-1/2 particles[17] the TBRME can be defined by the Hamiltonian

$$\mathbf{H}=\sum_{n,\sigma}\varepsilon_n |n,\sigma\rangle\langle n,\sigma| + \sum_{(n,m)(\sigma,\sigma')} V_{n,m}^{\sigma,\sigma'} |n,\sigma\rangle\langle m,\sigma'| \tag{2}$$

where n labels all the L^2 sites of the lattice and $\sigma=\pm 1/2$ is the spin index, while the second sum is taken over all nearest neighbor lattice pairs (n, m). The spin-independent random on-site potential ε_n denotes the diagonal disorder and is a uniformly distributed random variable chosen from a probability distribution of width W.

The nearest neighbor hopping matrix elements $V_{n,m}$ are randomly chosen 2×2 matrices describing spin rotation due to the SOC on every lattice bond (n, m). In the two-component spinor space they are represented by the quaternions

$$V_{n,m}=\begin{pmatrix} 1+i\mu V^z & \mu V^y+i\mu V^x \\ -\mu V^y+i\mu V^x & 1-i\mu V^z \end{pmatrix}_{n,m} \tag{3}$$

where μ denotes the SOC coupling and the V^x, V^y, and V^z defined for every (n, m) are real and independent random variables chosen from a uniform probability distribution on the interval $[1/2, +1/2]$. An alternative model of SOC has been introduced and studied by Ando.[18] There is a rigorous proof that the model of Eq. (2) has localized states if the disorder strength W is strong when compared to the SOC coupling μ.[19] The Anderson transition for a two-dimensional system with SOC was revealed in the numerical studies of refs. 17 and 18 and by an analytical renormalization group theory in ref. 20.

3. THE ORTHOGONAL CASE

3.1. $P(S)$ Distribution Function

We determine this curve by a direct numerical scaling attack of the level statistics in finite cubic lattices described by Eq. (1) of L^3 sites and Hamiltonian matrices of the same order. Our calculation relies on the numerical computation of the eigenvalues E_j in a very narrow window of states around $E=0$. The finite random matrices are diagonalized by the Lanczos algorithm and the large-L behavior is achieved by allowing the size L^3 to vary from 6^3 to 12^3 for many random configurations (see

Table I). The spacing function $P(S)$ can be numerically studied by considering instead of $E_{j+1} - E_j$ the distribution of the differences

$$\langle N(E_{j+1})\rangle - \langle N(E_j)\rangle = (E_{j+1} - E_j)\frac{\partial}{\partial E}\langle N(E)\rangle$$

where $\langle N(E)\rangle$ is the averaged integrated DOS at the energy E. This is a well-known unfolding procedure for the spectrum and it is required for the average level spacing Δ to remain equal to unity and $\langle \rho(E)\rangle$ constant in the chosen window.

Our numerical results for $P(S)$ are shown in Fig. 1. For the delocalized phase (Fig. 1a) for $W = 10 < W_c$ the $P(S)$ function is shown to approach

Table I. Results for $d = 3$ without SOC

Size (L)	Number of runs	Number of eigenvalues	γ	Δ	E (window)
$W = 10$					
6	60,000	592,755	0.092	0.054	0.0–0.55
8	10,000	106,676	0.085	0.023	0.0–0.25
10	7,205	78,000	0.090	0.012	0.0–0.13
12	13,980	160,807	0.084	0.007	0.0–0.08
$W = 16 \approx W_c$					
6	50,000	558,894	0.306	0.077	0.0–0.90
8	33,510	365,223	0.312	0.033	0.0–0.37
10	17,589	182,307	0.309	0.017	0.0–0.18
$W = 16.5 \approx W_c$					
6	88,121	960,727	0.333	0.079	0.0–0.90
8	10,000	106,115	0.352	0.033	0.0–0.37
10	15,515	156,922	0.346	0.017	0.0–0.18
12	18,274	194,945	0.349	0.010	0.0–0.11
$W = 30$					
6	45,468	448,120	0.760	0.131	0.0–1.40
8	10,000	106,557	0.808	0.055	0.0–0.64
10	14,088	142,195	0.837	0.028	0.0–0.31
12	15,278	145,995	0.891	0.016	0.0–0.17
$W = 12$ ($E_c \approx 7.8$)					
8	129,805	664,445	0.266	0.070	7.60–8.00
10	76,790	572,320	0.326	0.038	7.65–7.95
12	44,600	551,852	0.363	0.023	7.65–7.95

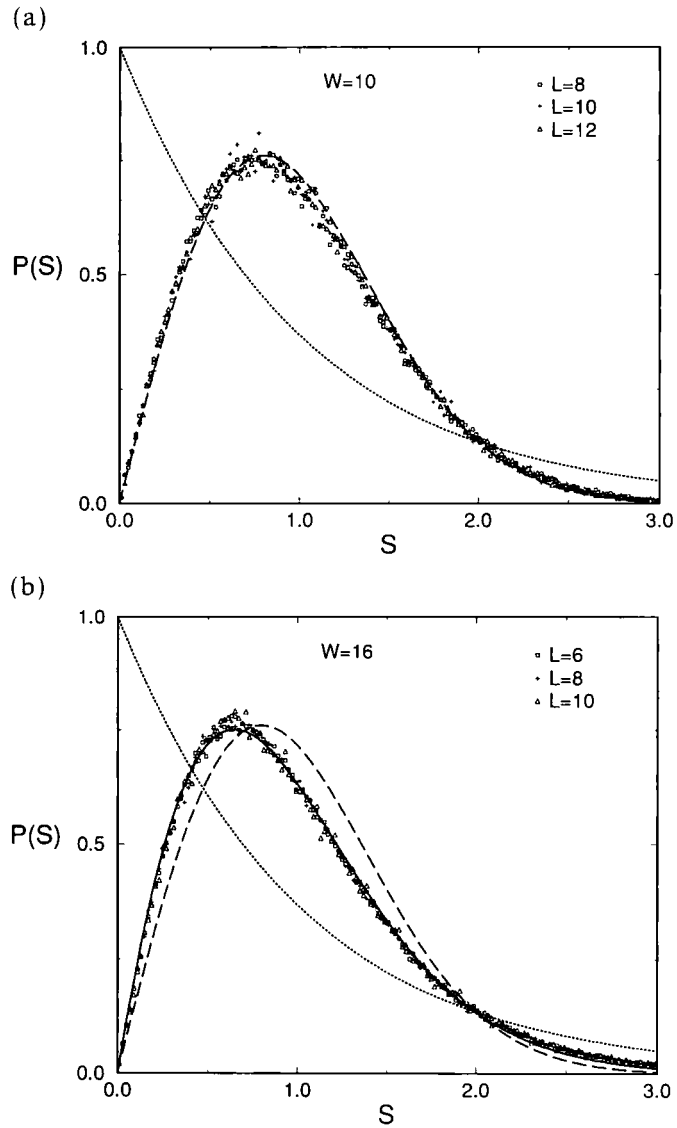

Fig. 1. The calculated level-spacing distribution function for the unfolded data for different system sizes and various disorder strengths corresponding to (a–d) $W = 10$, 16, 16.5, and 30, with the rest of the parameters taken from Table I. The broken line is the Wigner surmise (approached as $L \to \infty$ in the delocalized limit) and the dotted line is the Poisson law (approached as $L \to \infty$ in the localized limit). The critical scale invariant curve is shown in cases (b) and (c) together with the corresponding analytical best fit from Eq. (4) with $B \approx 2.32$, $A \approx 1.30$, and $\alpha \approx 1.45$ for $W = 16.0$ and $B \approx 2.46$, $A \approx 1.38$, and $\alpha \approx 1.38$ for $W = 16.5$, respectively. (e) Plot of the critical $P(S)$ when the mobility edge lies outside the band center at $E_c \approx 7.8$ for $W = 12$, together with the analytical best fit of Eq. (4) with $B \approx 2.52$, $A \approx 1.41$, and $\alpha \approx 1.37$.

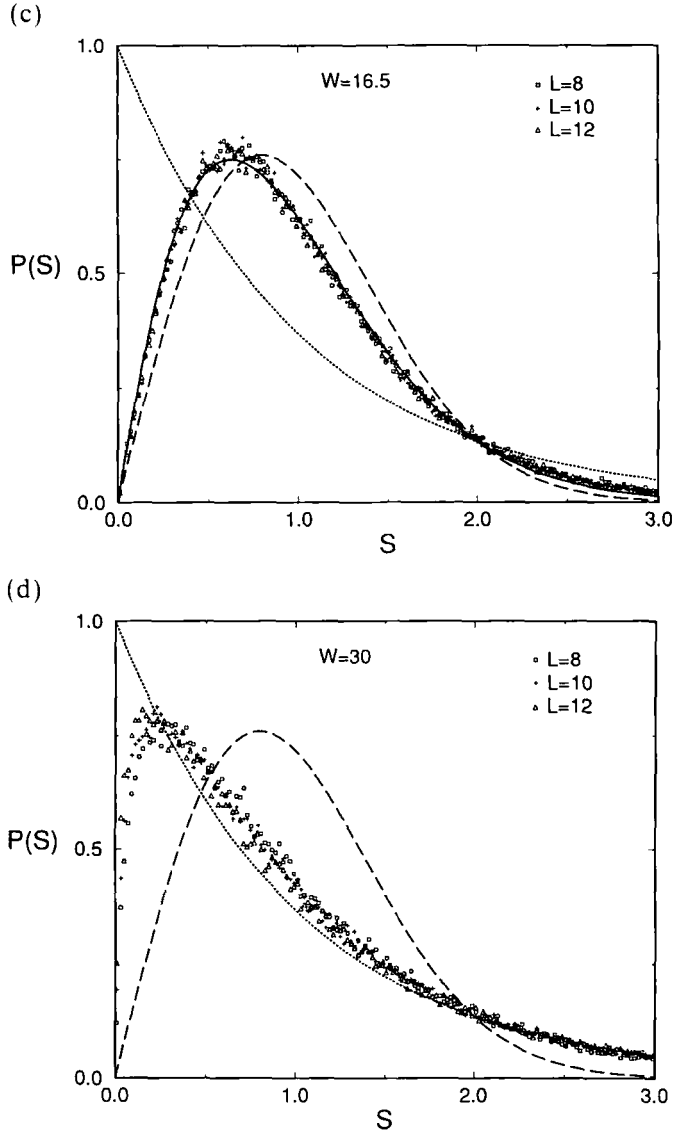

Fig. 1 *(Continued)*

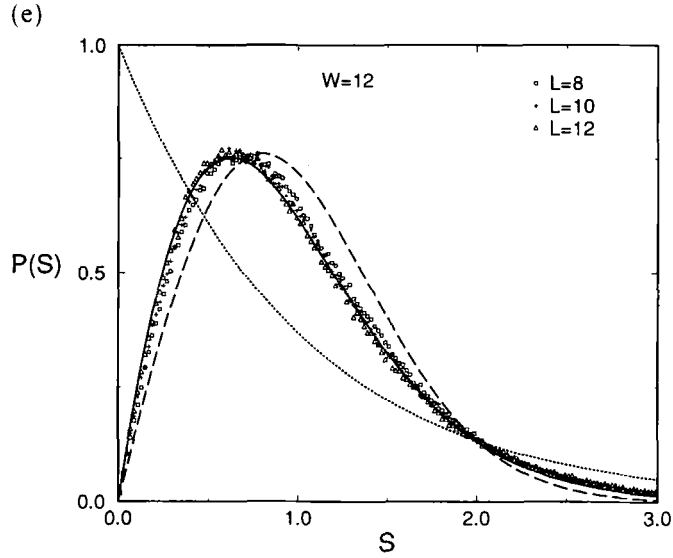

Fig. 1 *(Continued)*

rapidly the Wigner surmise law as a function of the system size. In the localized phase for $W=30>W_c$ (Fig. 1d) we find that our results resemble a displaced Wigner-like curve, but they show a tendency to move toward the Poisson distribution as the size L increases, although only asymptotically for sizes much larger than the localization length. At the mobility edge ($E_c=0$ in this case) we obtain within numerical errors a size-independent universal scale invariant $P(S)$ function which interpolates between the Wigner and Poisson limits.[10,21] The results for the critical case are shown in Figs. 1b and 1c for the values $W=16$ and $W=16.5$, respectively. The scaling parameter γ introduced in ref. 10 is shown (Table I) to remain approximately constant at the critical point. The need for considering two estimates for the critical disorder arises from the fact that an uncertainty exists; for example, from a scaling approach using level statistics a W_c value was obtained that was slightly smaller than 16.5 obtained by the transfer matrix method.[22] Despite the various sources of numerical errors, already apparent in Fig. 1b and 1c a reasonable overall fit of the data to the suggested analytical interpolation form[12-15]

$$P(S)=BS\exp(-AS^{\alpha}) \tag{4}$$

gave $\alpha\approx 1.38$ and 1.45 (see also ref. 21) for $W=16.5$ and 16, respectively. We observe that the exponent α is close to the estimate $1+1/(vd)=4/3$

predicted from the theory[12–15] where the localization length critical exponent is $\nu = 1$ taken from the first-order ε expansion estimate and $d = 3$ is the space dimensionality. The well-established $\nu \approx 1.4$ numerical transfer matrix scaling value gives slightly smaller values than 4/3. The χ^2 values for the critical $P(S)$ gave small values (around 2), which suggest good quality of the corresponding fits. However, fits of the less accurate data in the tail of the critical $P(S)$ distribution gave values for α closer to unity, which could imply an almost Poissonic behavior for very large S.[21]

In order to check the validity of the asymptotic critical curve of Eq. (4) we also consider restricted energy ranges near the mobility edge when it lies outside the band center $E = 0$ for a fixed amount of disorder. In Fig. 1e we show our scaling results for the case of $W = 12$ together with the analytical fit of Eq. (1), near the mobility edge, which lies at $E_c = 7.8 \pm 0.1$.[16] Although the main features of this distribution are also established by the fit of Eq. (4) which gave $\alpha \approx 1.37$, it must be pointed out that from the quality of the fit we cannot exclude an even more complicated form of the critical $P(S)$.

3.2. Number Variance $\langle (\delta N)^2 \rangle$

We have also obtained results for $\langle (\delta N(E))^2 \rangle = \langle N(E)^2 \rangle - \langle N(E) \rangle^2$, which characterizes the stiffness of the spectrum by measuring the fluctuations of the number of eigenvalues $N(E)$ in a given energy window E. In Fig. 2a we plot $\langle (\delta N(E))^2 \rangle$ versus $\langle N(E) \rangle$, for eigenvalues obtained in the energy windows defined in Table 1, together with the logarithmic Wigner–Dyson GOE limit.[6] We can again distinguish three cases corresponding to the metal, insulator, and critical point, respectively. In the metallic case ($W = 10$) the results are seen to rapidly reach the analytic Wigner expression for small $\langle N(E) \rangle$, starting to deviate at a value of $\langle N(E_T) \rangle$ which defines the Thouless energy E_T for the finite system. In the localized phase ($W = 30$), instead, our result slowly approach the Poisson limit $\langle (\delta N(E))^2 \rangle = \langle N(E) \rangle$ (see also Fig. 2b) which implies uncorrelated levels.

In the critical case the data for different system sizes converge, at least for the smaller $\langle N(E) \rangle$, to a universal curve. From recent analytic results[15] one expects the asymptotic law

$$\langle (\delta N(E))^2 \rangle = A \langle N(E) \rangle + B \langle N(E) \rangle^{2-\alpha}, \qquad A, B = \text{const} \tag{5}$$

for $\langle N(E) \rangle \gg 1$, which also includes the dominant linear term. A fit of the data to the non-linear part alone, believed to be due to a sum rule which was shown to be invalid for the infinite system,[15] previously gave α values not very far from unity, in agreement with an almost exponential tail[21] for

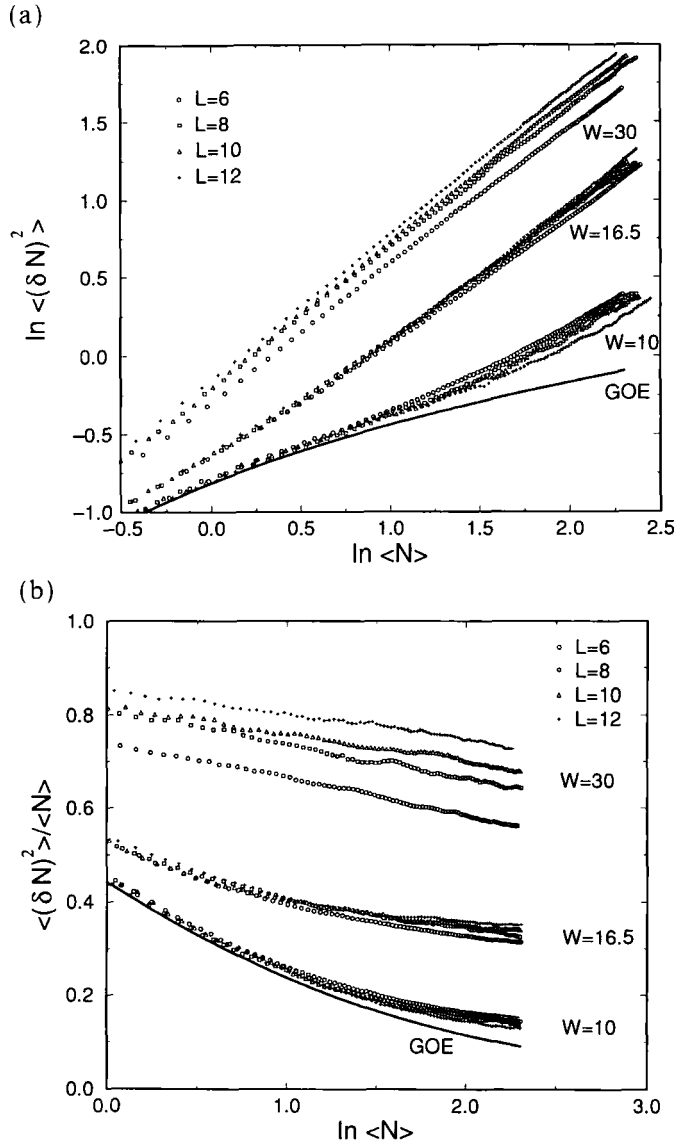

Fig. 2. (a) The calculated number variance distribution function for the same parameters as in Fig. 1 taken from Table I. The corresponding continuous line is the result for the Gaussian orthogonal ensemble (GOE), which should apply to the metallic phase. It must be also noted that for the localized ($W=30$) case the data for the different system sizes go toward the Poisson limit $\langle(\delta N)^2\rangle = \langle N\rangle$. (b) The same as in (a), but the data are displayed by plotting the ratio $\langle(\delta N)^2\rangle/\langle N\rangle$ vs. $\langle N\rangle$, so that the Poisson limit is 1. (c) The same as in (a), but including the case of $W_c = 16$ instead of 16.5.

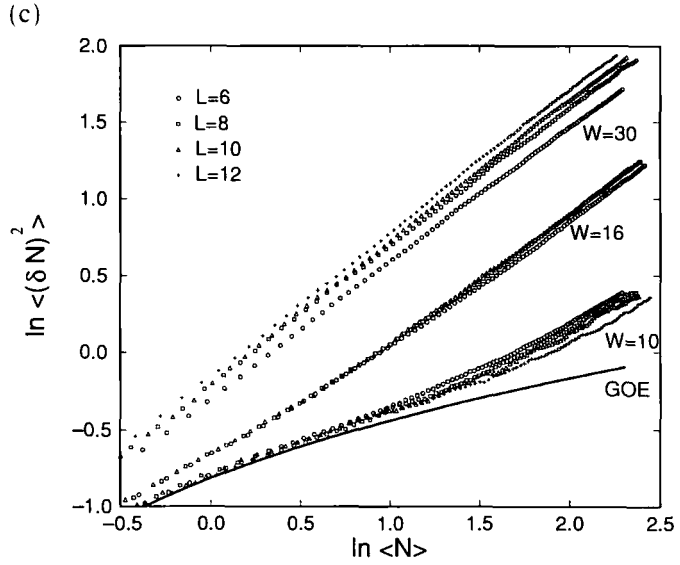

Fig. 2 *(Continued)*

the $P(S)$ if $S \gg 1$. In Fig. 2b we plot our data in a different way in order to show the $\langle N \rangle$ dependence of the ratio $\langle (\delta N(E))^2 \rangle / \langle N(E) \rangle$, which varies weakly with $\langle N \rangle$ and approaches a constant ratio A in the critical case. Moreover, our main conclusions drawn from Figs. 2a and 2b remain valid by taking $W = 16$ as the critical disorder (Fig. 2c) and also near the mobility edge when it lies outside the band center.

3.3. Two-Point Correlation Function $K_2(\epsilon)$

The two-point density–density correlation is a function of the relative distance ε between any two eigenvalues in units of Δ, not necessarily nearest neighbors, via

$$K_2(\varepsilon) = 1 - \frac{\langle \rho(E)\, \rho(E+\varepsilon) \rangle}{\langle \rho(E) \rangle \langle \rho(E+\varepsilon) \rangle} \tag{6}$$

where $\rho(E)$ is the one-electron DOS for one realization of the disorder and $\langle \ldots \rangle$ denotes ensemble average over many realizations. $K_2(\varepsilon)$ as defined in

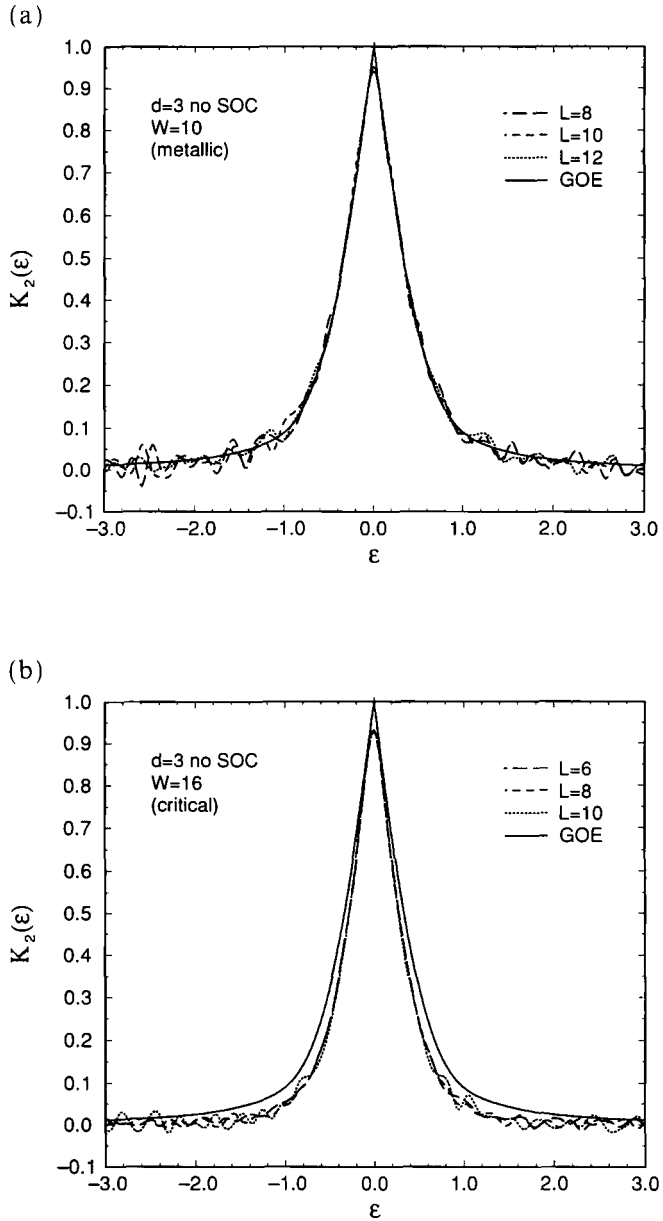

Fig. 3. The calculated two-point density correlation function for different system sizes in a log–log plot for various disorder strengths and parameters from Table I. The corresponding continuous line is the result for the Gaussian orthogonal ensemble (GOE), which applies to the metallic phase [Eq. (7)]. (b,c) The critical intermediate curve.

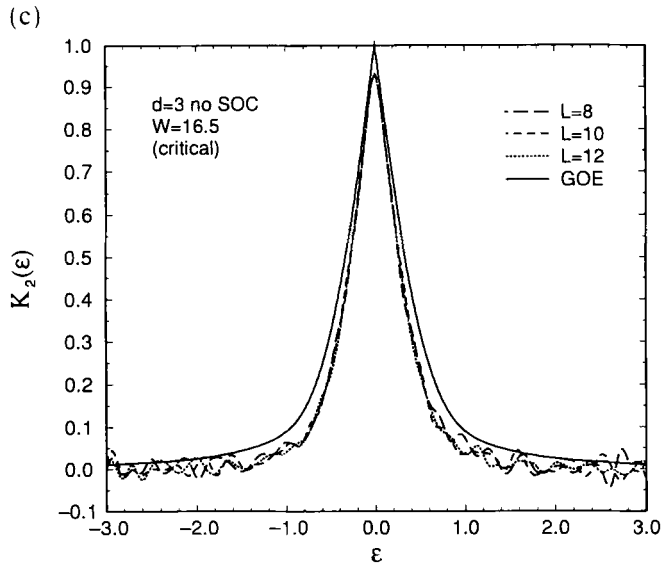

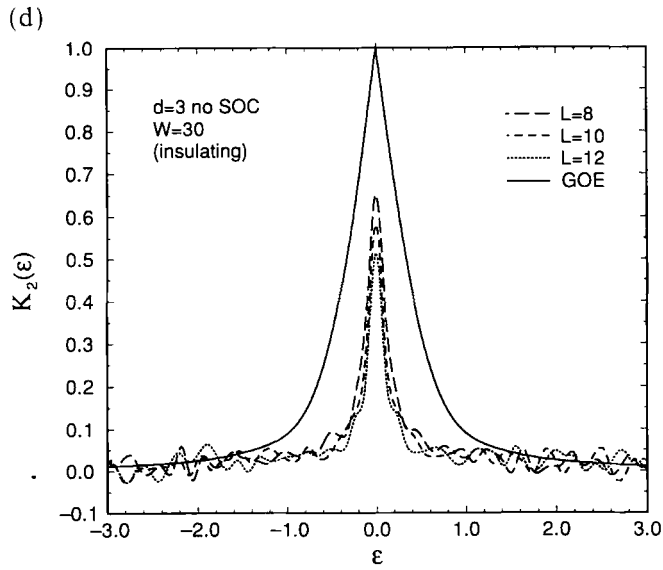

Fig. 3 *(Continued)*

Eq. (6) measures departures from the uncorrelated systems and for a metallic system we expect the GOE result[6]

$$K_2(\varepsilon) = \left(\frac{\sin \pi\varepsilon}{\pi\varepsilon}\right)^2 - \left(\int_0^{\pi\varepsilon} \frac{\sin y}{y}\, dy - \frac{\pi}{2}\right)\left(\frac{\cos \pi\varepsilon}{\pi\varepsilon} - \frac{\sin \pi\varepsilon}{(\pi\varepsilon)^2}\right), \qquad \varepsilon > 0 \quad (7)$$

with $K_2(-\varepsilon) = K_2(\varepsilon)$ and $K_2(0) = 1$. For the insulating phase the correlations vanish, so that for $L \to \infty$ the limit

$$K_2(\varepsilon) = 0 \quad (8)$$

should be reached. $K_2(\varepsilon)$ can be directly computed from the numerical data, within the chosen energy window, by fixing a finite small energy box for the origin E (of width 0.1Δ) and measuring the reduced probability via Eq. (6) in another box at a distance $E + \varepsilon$. In order to improve the statistics we considered several values for the origin E and performed an average over the statistical ensemble. The results shown are obtained for the unfolded levels, although the averaged DOS $\langle \rho(E) \rangle$ is already almost constant in the chosen energy window.

The numerical data for $K_2(\varepsilon)$ are displayed in Fig. 3. In the metallic phase they almost coincide with the GOE result, particularly for small ε (Fig. 3a), and for the insulator there is a slow crossover toward the zero correlation limit for increasing system size (Fig. 3d). In Fig. 3b and 3c we show intermediate scale-invariant curves which are obtained at the critical point. We should emphasise that $K_2(\varepsilon)$ should fall with an inverse square power law ε^{-2} for the metal and according to the statistical theory of[12-15] in the critical case $K_2(\varepsilon) \propto \varepsilon^{-\alpha}$, with the previously found exponent α also governing this asymptotic large-ε decay. We cannot obtain α from our data because our window is too small to reach the very large ε regime.

4. THE SYMPLECTIC CASE

4.1. The Metal–Insulator Transition

Before we undertake the level statistical study for the two-dimensional symplectic system we perform transfer matrix calculations[23] in order to determine the critical disorder value for energies close to the band center. We consider very long strips of length 5×10^5 to 10^6 and vary the perpendicular width M. For fixed M we obtain the spectrum of the converged Lyapunov exponents γ_j with $j = 1, 2, \ldots, M$ from the corresponding random transfer matrix product.[16] Since all the states are localized for the finite system in the adopted quasi-one-dimensional strip geometry, the pairwise

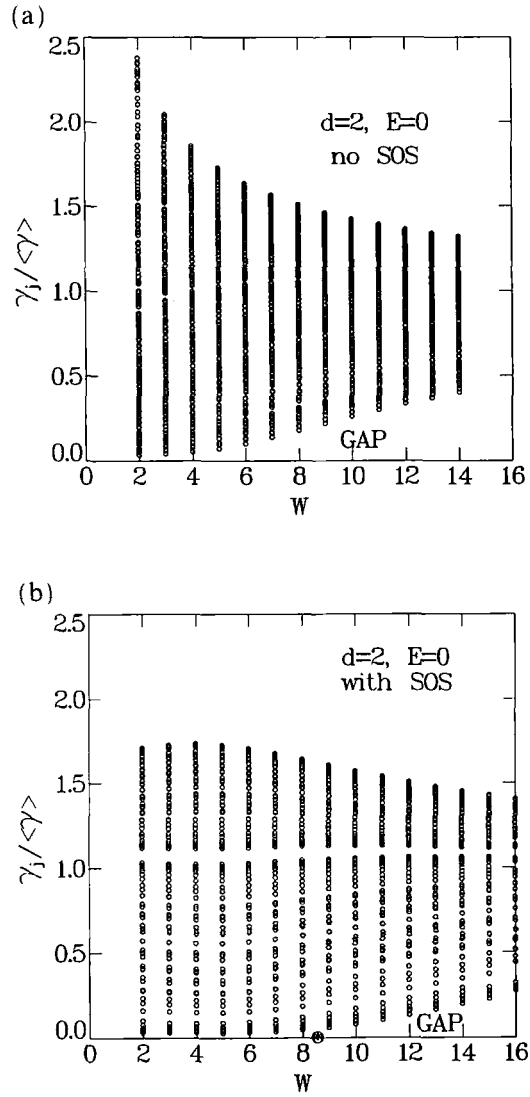

Fig. 4. The Lyapunov exponents γ_j, $j = 1, 2, ..., M$, for two-dimensional strip systems with various values of the strip width M, normalized by their respective mean value $\langle\gamma\rangle = (1/M)\sum_j \gamma_j$. (a) A gap in the Lyapunov spectrum opens up for any W without SOC ($\mu = 0$) and (b) only for $W > W_c$ for finite SOC ($\mu = 2$), indicating the transition in the latter case. The asterisk denotes W_c.

degenerate positive exponents γ_j are different from zero. Their inverses γ_j^{-1} define a hierarchy of localization lengths and we focus on the smallest exponent γ_1, which corresponds to the dominant transmission channel with the largest localization length $\xi_M = \gamma_1^{-1}$. If the states are localized, the localization length is obtained from the limit $\xi = \lim_{M \to \infty} \xi_M$ while for extended states it is expected to diverge ($\xi \to \infty$). The renormalized length ξ_M/M should decrease or increase by increasing M for the localized and extended cases, respectively. At the critical point $W = W_c$ we obtain a scale-invariant fixed-point value $(\xi_M/M)^*$ for every M only for the $\mu = 2$ case, which confirms the presence of an Anderson transition for finite SOC in $d = 2$ with the absence of a transition for $\mu = 0$. The critical disorder value was found by this method to be $W_c = 8.55 \pm 0.05$.[23]

In order to display the transition in Figs 4a and 4b we present all the Lyapunov exponents γ_j for various values of M normalized dividing by their respective mean value $\langle \gamma \rangle = (1/M) \sum_j \gamma_j$. It is seen that the minimum exponent whose inverse gives ξ_M approaches zero for $W < W_c$ and remains finite for $W > W_c$ when $\mu = 2$, while for $\mu = 0$ it is finite for any W. In other words, a gap in the corresponding Lyapunov spectrum which includes both the positive and negative exponents opens up in the middle of the spectrum having asymptotic width $2/\xi$ for any W without SOC and only for $W > W_c$ for finite SOC, indicating the transition in the latter case. The critical disorder value in the finite SOC case is also shown in Fig. 4b.

4.2. $P(S)$ Distribution Function

We are now in a position to derive the level statistics for finite squared lattice systems with SOC of strength $\mu = 2$ described by Eq. (2). We numerically compute the eigenvalues E_j around $E = 0$ for lattices of L^2 sites and many random configurations by ignoring Kramer's degeneracy. The finite-size $(2L^2) \times (2L^2)$ symplectic random matrices are diagonalized and the large-L behavior is achieved by allowing the matrix size to vary from $2 \cdot 8^2$ to $2 \cdot 16^2$ (see Table II). We again considered the unfolded spacings $\langle N(E_{i+1}) \rangle - \langle N(E_i) \rangle$, where the averaged IDOS $\langle N(E) \rangle$ is computed within the adopted energy range at a few points and then found at many points by cubic interpolation, in order to obtain the unfolded levels $\langle N(E_i) \rangle$. The $P(S)$ distribution with $S = \langle N(E_{i+1}) \rangle - \langle N(E_i) \rangle$ satisfies the constant DOS requirement $\Delta = 1$.

We find that as L increases, our results move toward the corresponding Wigner surmise in the delocalized phase ($W < W_c$) and the Poisson law in the localized limit ($W > W_c$), respectively. In Fig. 5a for the delocalized case of $W = 6$ the $P(S)$ function is shown to move toward the symplectic Wigner surmise, while in the localized phase for $W = 12$ (Fig. 5c) our

Table II. Results for $d=2$ with SOC of Strength $\mu=2$

Size (L)	Number of runs	Number of eigenvalues	Δ	E (window)
$W=6$				
8	35,000	1,220,273	0.171	−3.0 to 3.0
12	11,000	862,889	0.076	−3.0 to 3.0
16	19,446	2,710,937	0.043	−3.0 to 3.0
$W=8.55\approx W_c$				
8	10,000	309,531	0.193	−3.0 to 3.0
12	9,000	627,330	0.086	−3.0 to 3.0
16	14,273	1,767,874	0.048	−3.0 to 3.0
$W=12$				
8	40,378	1,048,029	0.229	−3.0 to 3.0
12	13,023	760,821	0.102	−3.0 to 3.0
16	16,683	1,732,856	0.058	−3.0 to 3.0

system sizes are too small with respect to the corresponding localization lengths to reach the Poisson limit, although the data clearly have a tendency to move toward the Poisson distribution as a function of the system size. The speed of approach can be improved if the system sizes become larger or the adopted disorder stronger.

At the mobility edge there also should exist an L-independent universal scale-invariant $P(S)$ function approximated by the formula

$$P(S)=BS^4\exp(-AS^\alpha) \tag{9}$$

which interpolates between the two limits. Our data for this intermediate $P(S)$ are shown in Fig. 5b and it should be noted that they give the profile of a function which has most of the features already established for the three-dimensional spinless critical case (Figs 1b, 1c, and 1e), but with a quartic behavior ($\beta=4$) for small S due to the symplectic nature of the random matrices. The critical $P(S)$ is closer to the GSE result and passes very near the point $S\approx 1.63$ where the Wigner and the Poisson cross. Previous overall fit of the data to the suggested analytical form of Eq. (9) gave $B\approx 22.35$, $A\approx 3.02$, and for the exponent $\alpha\approx 1.60\pm 0.05$.[23] This value is very different from the estimate $1+1/(vd)$, which if adopted would imply $v\approx 0.83$ in $d=2$. Although the computed $\chi^2\approx 13$ for $L=16$ and $\chi^2\approx 14$ for $L=12$ are less than the expected values, suggesting a good fit for the smaller S, we cannot exclude a different, more complicated form of

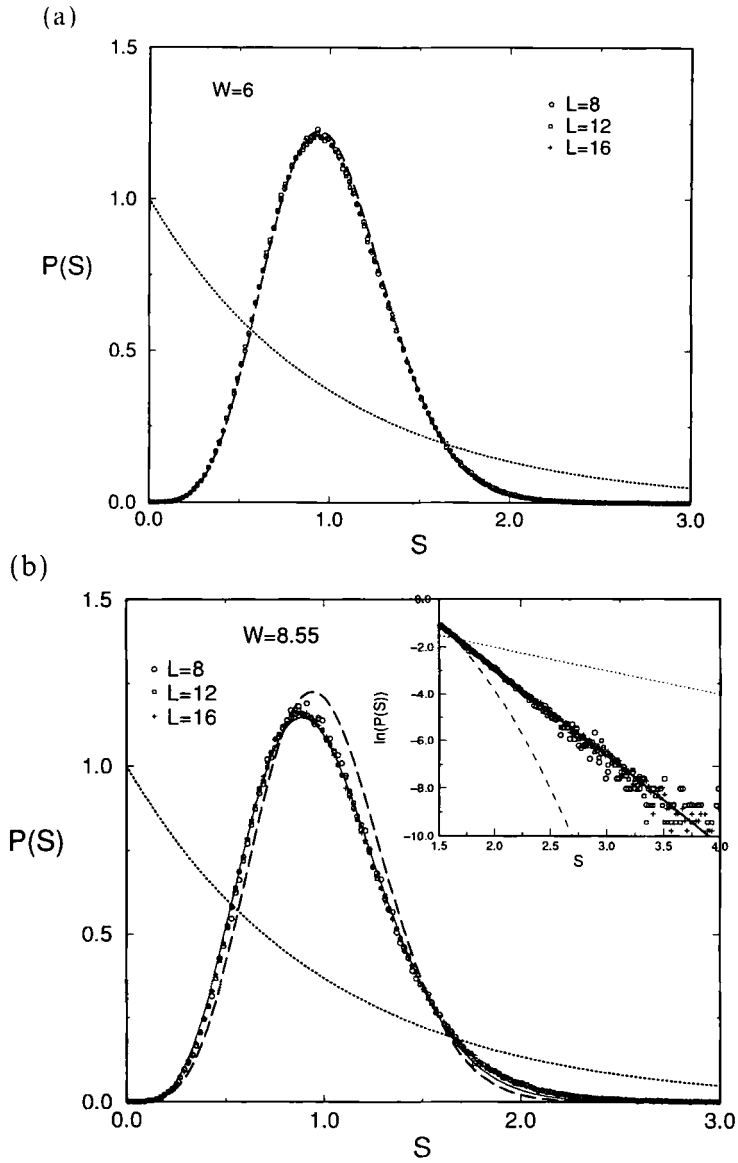

Fig. 5. The calculated level-spacing distribution function for disorder strengths corresponding to (a–c) $W = 6$, 8.55, and 12 with the parameters from Table II. The broken line is the Wigner surmise (approached as $L \to \infty$ in the delocalized limit) and the dotted line is the Poisson law (approached as $L \to \infty$ in the localized limit). The critical scale-invariant curve is shown in (b) with the corresponding best fit to Eq. (9). Our results for the tail of the critical $P(S)$ are displayed in the inset of (b).

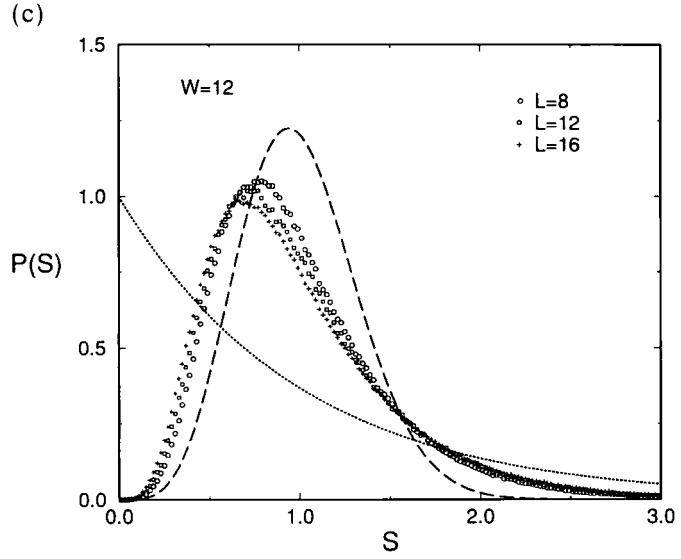

Fig. 5 *(Continued)*

the critical $P(S)$. For this purpose we have also attempted a linear fit of $\ln P(S)$ in the far tail (see inset), where our data have bigger errors. It is seen that a simple exponential $P(S) \propto \exp(-AS)$ can also provide a good fit for the region $1.5 < S < 4.0$ and for the largest size considered we obtain $A \approx 3.71$ with $\chi^2 \approx 9$.

4.3. Number Variance $\langle (\delta N)^2 \rangle$

Our scaling results for the number variance $\langle (\delta N(E))^2 \rangle$ vs. $\langle N(E) \rangle$ are shown in Fig. 6. We can again distinguish three regimes corresponding to the metal, insulator, and critical point, respectively. In the metallic case the results are close to the analytic symplectic Wigner expression for small $\langle N(E) \rangle$ and the point of deviation gives the Thouless energy E_T, which defines a conductance smaller than that for the corresponding $d = 3$ case. In the localized phase the scaling data should slowly approach the $\langle (\delta N(E))^2 \rangle = \langle N(E) \rangle$ Poisson limit. However, we find a much slower approach to this limit when compared to $d = 3$ and our data show an intermediate nonlinear growth $\langle N(E) \rangle^{3/4}$. In the critical regime the data for different system sizes converge within numerical accuracy and for the larger $\langle N(E) \rangle$ to the same asymptotics as for the localized case.

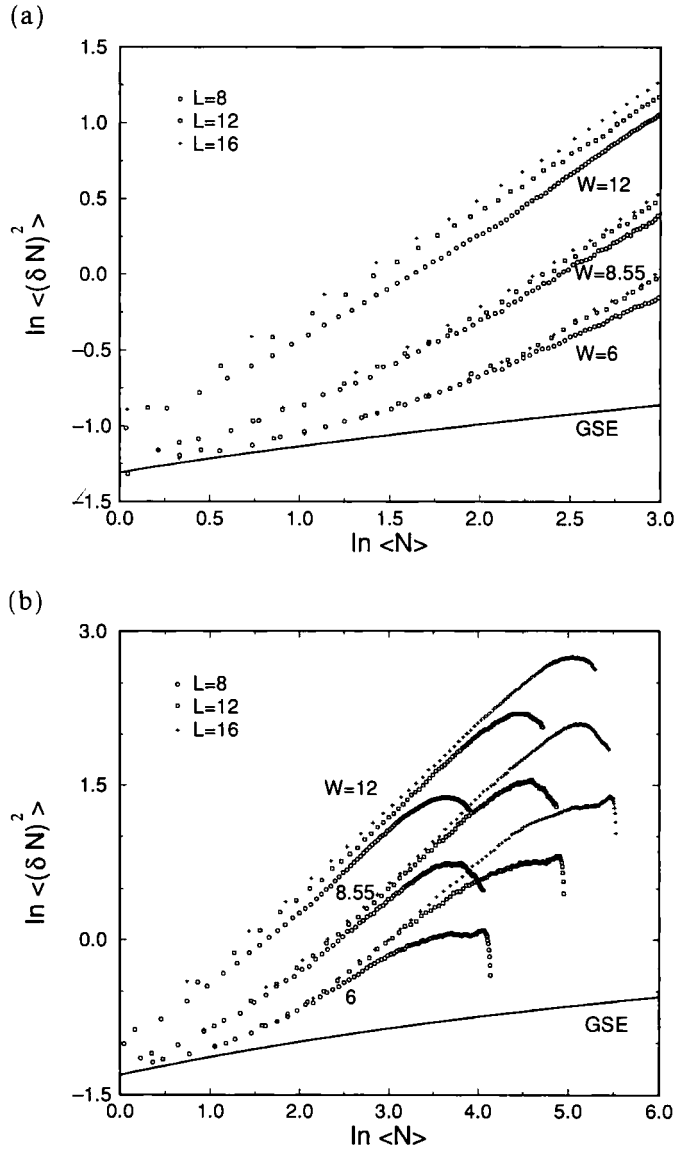

Fig. 6. The calculated number variance distribution function for the same parameters as in Fig. 5 from Table II. The corresponding continuous line is the result for the Gaussian symplectic ensemble (GSE), which should apply to the metallic phase.

In Fig. 6b we plot the raw data before unfolding for the number variance in the whole energy range, up to the band edges, starting from $E=0$. We also see the intermediate nonlinear growth for large $\langle N(E)\rangle$, which is probably a finite-size effect due to the choices of disorder made and the rather small sizes considered. This feature should disappear in the aymptotic limit, leading eventually to a linear Poisson law also for $d=2$.

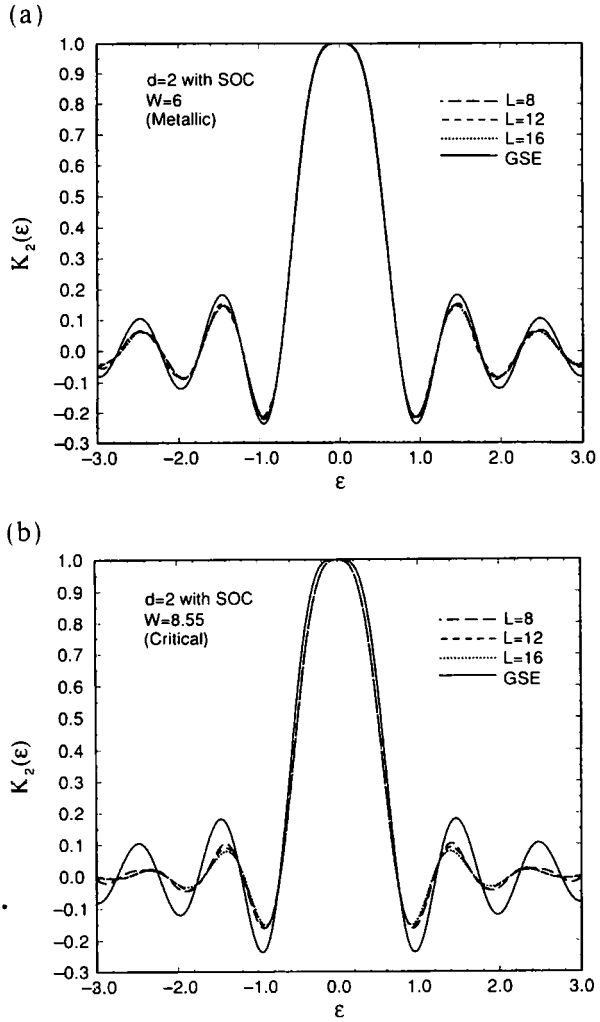

Fig. 7. The calculated two-point density correlation function for different system sizes in a log–log plot for various disorder strengths and parameters from Table II. The corresponding continuous line is the GSE result [Eq. (10)], which should apply to the metallic phase.

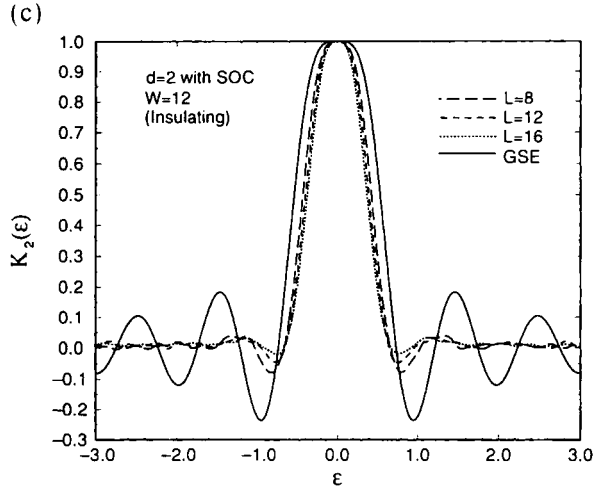

Fig. 7 *(Continued)*

4.4. Two-Point Correlation Function $K_2(\epsilon)$

The density correlation function for the GSE is

$$K_2(\varepsilon) = \left(\frac{\sin 2\pi\varepsilon}{2\pi\varepsilon}\right)^2 - \left(\frac{\cos 2\pi\varepsilon}{2\pi\varepsilon} - \frac{\sin 2\pi\varepsilon}{(2\pi\varepsilon)^2}\right)\int_0^{2\pi\varepsilon} \frac{\sin y}{y}\, dy \tag{10}$$

with $K_2(0) = 1$, and this result is expected to hold in the metallic phase. In Fig. 7a we observe a slow crossover of $K_2(\varepsilon)$ toward the GSE result and in Fig. 7c toward the zero value, indicating the absence of correlations in the latter case. It must be pointed out that in the localized case from the adopted disorder $W = 12$ and the L values considered our data cannot reliably demonstrate the zero-correlation limit. For example, at ε close to 0 correlations still remain in this case, which is similar to the linear $P(S)$ found for small S for the localized case shown in Fig. 5c. These features are clearly finite-size effects and K_2 for small ε will decrease if larger sizes are taken, eventually approaching zero for the infinite system. At the critical point an intermediate curve is shown in Fig. 7b which also differs from its $d = 3$ analogue, since the small-ε behavior follows more closely the corresponding RMT result in the form of GSE when compared to the corresponding GOE case.[23]

5. DISCUSSION AND CONCLUSIONS

We have presented a complete level statistical study, including the spectral rigidity which has further physical consequences, for two time-reversal invariant TBRMEs defined in two- and three-dimensional lattices with and without SOC, respectively. The metal–insulator transition is also demonstrated in the finite SOC case which corresponds to the symplectic universality class in $d=2$. Numerical results for finite lattices of different sizes are derived in both cases for the nearest level spacing distribution function $P(S)$, the number variance $\langle(\delta N)^2\rangle$ and the two-point correlation function $K_2(\varepsilon)$. In the metallic regime ($W < W_c$) for small energies less than the Thouless energy E_T the results are shown to be closely approximated by the GOE and GSE for the two statistical ensembles, respectively. This confirms previous analytical results for weakly disordered small metallic systems,[24] where level correlations similar to the quantum chaotic GOE and GSE results are found, suggesting a universal validity of the RMT for disordered metals. In the strong-disorder limit ($W > W_c$) the electrons localize and the correlations between the levels diasappear, leading to independent Poisson statistics. However, this is more difficult to obtain numerically for small sizes, although the corresponding trends are clearly demonstrated. We have also obtained new curves at the critical boundary ($W = W_c$) which are discussed with respect to recent theories.

In conclusion, we have shown by numerical scaling methods many interesting level statistical fluctuation properties for disordered metals in the tight-binding approximation. These systems provide physical realizations of the orthogonal and symplectic symmetries defined within the usual Wigner–Dyson RMT and offer the possibility of estimating measurable universal symmetry dependences. We have confirmed that the orthogonal and symplectic systems studied display metallic behavior described by the GOE and GSE, respectively, but at the disorder-induced metal–insulator transition the two ensembles show certain differences particularly for $\langle(\delta N)^2\rangle$ and $K_2(\varepsilon)$. An obvious extension of the present work is to consider the three-dimensional SOC case in order to check the suggested universality, especially for the critical case, or other symmetry-breaking factors such as the presence of Andreev scattering.[25]

ACKNOWLEDGMENT

This work was supported in part by a ΠΕΝΕΔ Research Grant of the Greek Secretariat of Science and Technology and from EEC, contract HCM-CHRX-CT93-0126.

REFERENCES

1. B. Kramer and A. MacKinnon, *Rep. Prog. Phys.* **56**:1469 (1993), and references therein.
2. P. W. Anderson, *Phys. Rev.* **109**:1492 (1958).
3. E. Abrahams, P. W. Anderson, D. C. Licciardello, and T. V. Ramakrishnan, *Phys. Rev. Lett.* **42**:673 (1979).
4. S. Hikami, A. I. Larkin, and Y. Nagaoka, *Prog. Theor. Phys.* **63**:707 (1980).
5. E. P. Wigner, *Ann. Math.* **53**:36 (1951); **62**:548 (1955); **65**:203 (1957); C. E. Porter, in *Statistical Theories of Spectra: Fluctuations* (Academic Press, New York, 1965).
6. O. Bohigas, In *Chaos and Quantum Physics*, M. -J. Giannoni, A. Voros, and J. Zinn-Justin eds. (North-Holland, Amsterdam, 1991).
7. F. Haake, *Quantum Signatures of Chaos* (Springer, Berlin, 1991).
8. B. L. Altshuler and B. I. Shklovskii, *Zh. Eksp. Teor. Fiz.* **91**:220 (1986) [*Sov. Phys. JETP* **64**:127 (1986)].
9. B. L. Altshuler, I. Kh. Zharekeshev, S. A. Kotochigova and B. I. Shklovskii, *Zh. Eksp. Teor. Fiz.* **94**:343 (1988) [*Sov. Phys. JETP* **67**:625 (1988)].
10. B. I. Shklovskii, B. Shapiro, B. R. Sears, P. Labrianides, and H. B. Shore, *Phys. Rev. B* **47**:11487 (1993).
11. S. N. Evangelou, *Prog. Theor. Phys.* **116**:319 (1994); S. N. Evangelou, *Phys. Rev. B* **39**:12895 (1989).
12. A. G. Aronov, V. E. Kravtsov, and I. V. Lerner, *Pis 'ma Zh. Eksp. Teor. Fiz.* **59**:39 (1994); *JETP Lett.* **59**:40 (1994).
13. V. E. Kravtsov, I. V. Lerner, B. L. Altshuler, and A. G. Aronov, *Phys. Rev. Lett.* **72**:888 (1994).
14. A. G. Aronov, V. E. Kravtsov, and I. V. Lerner, *Phys. Rev. Lett.* **74**:1174 (1995).
15. V. E. Kravtsov and I. V. Lerner, *Phys. Rev. Lett.* **74**; 2563 (1995); *J. Phys. A: Math. Gen.* **28**:3623 (1995).
16. B. Kramer, K. Broderix, A. MacKinnon, and M. Schreiber, *Physica A* **167**:163 (1990).
17. S. N. Evangelou and T. A. L. Ziman, *J. Phys. C: Solid State Phys.* **20**:L235 (1987).
18. T. Ando, *Phys. Rev. B* **40**:5325 (1989).
19. J. Bellisard, D. R. Grembel, F. Martinelli, and E. Scopolla, *Phys. Rev. B* **33**:641 (1986).
20. A. Kawabata, *J. Phys. Soc. Japan* **57**:1717 (1988); *Physica A* **167**:279 (1990).
21. S. N. Evangelou, *Phys. Rev. B* **49**:16805 (1994).
22. I. Kh Zharekeshev and B. Kramer, *Phys. Rev. B* **51**:17239 (1995).
23. S. N. Evangelou, *Phys. Rev. Lett.* **75**:2550 (1995).
24. K. B. Efetov, *Zh. Eksp. Teor. Fiz.* **83**:833 (1982) [*Sov. Phys. JETP* **56**:467 (1982)].
25. J. T. Bruun, S. N. Evangelou, and C. J. Lambert, *J. Phys.: Condens. Matter* **7**:4033 (1995).